# Spo76p Is a Conserved Chromosome Morphogenesis Protein that Links the Mitotic and Meiotic Programs

Diana van Heemst,*§ Françoise James,*
Stefanie Pöggeler,† Véronique Berteaux-Lecellier,*
and Denise Zickler*‡
*Institut de Génétique et Microbiologie
UMR 8621
Université Paris-Sud
91405 Orsay Cedex
France
†Lehrstuhl für Allgemeine Botanik
Ruhr Universität
D-44780 Bochum
Germany

## Summary

Spo76p is conserved and related to the fungal proteins Pds5p and BIMD and the human AS3 prostate proliferative shutoff-associated protein. Spo76p localizes to mitotic and meiotic chromosomes, except at metaphase(s) and anaphase(s). During meiotic prophase, Spo76p assembles into strong lines in correlation with axial element formation. As inferred from *spo76-1* mutant phenotypes, Spo76p is required for sister chromatid cohesiveness, chromosome axis morphogenesis, and chromatin condensation during critical transitions at mitotic prometaphase and meiotic midprophase. Spo76p is also required for meiotic interhomolog recombination, likely at postinitiation stage(s). We propose that a disruptive force coordinately promotes chromosomal axial compaction and destabilization of sister connections and that Spo76p restrains and channels the effects of this force into appropriate morphogenetic mitotic and meiotic outcomes.

## Introduction

Chromosome morphogenesis involves a number of basic stages, elucidated for both the mitotic cycle and meiosis. Chromosomes replicate, with concomitant establishment of sister cohesion (e.g., Uhlmann and Nasmyth, 1998). At early–mid prophase, chromosomes are still relatively extended; from late prophase and into metaphase, higher order axial condensation (coiling/folding) arises, yielding chromosomes compact enough for separation at the ensuing division (reviewed in Koshland and Strunnikov, 1996).

The meiotic version of this program involves several specialized differentiations. First, at early–mid prophase, chromosomes are highly ordered, with sister chromatids organized into parallel, cooriented linear arrays of loops, closely conjoined at their bases by the axial element (AE) (e.g., Moens and Pearlman, 1988).

Second, chromosomes remain in this extended configuration for a long time, presumably to accommodate the complex events of meiotic interhomolog interactions (pairing, recombination, and synaptonemal complex [SC] formation). Third, meiotic prophase includes the structurally differentiated attachment of chromosome ends to the nuclear envelope plus programmed migration of those ends into and out of the bouquet configuration (review in Zickler and Kleckner, 1998). These events are all completed by the end of pachytene. The meiosis-specific structures (AE/SC) then disintegrate, and after a transient diffuse stage, chromosomes compact progressively into their metaphase conformation just as during the corresponding mitotic stage (review in von Wettstein et al., 1984). Notably, also, meiotic prophase is followed by two rounds of chromosome segregation. During mitosis, sister chromatid connections lapse first along the chromatid arms at the metaphase/anaphase transition and then, at the onset of anaphase, in centric regions. The same two phases occur during meiosis except that arm connections lapse at the first meiotic division while centric connections lapse only at the second division (review in Nicklas et al., 1995; Moore and Orr-Weaver, 1998).

Mechanisms responsible for the basic processes of chromosome morphogenesis and for specializations during the meiotic program are not yet fully understood. Insights into mitotic chromosome metabolism, and especially the essential process of sister chromatid cohesion, have emerged recently from genetic and cytogenetic studies in budding and fission yeasts and by biochemical approaches in *Xenopus* egg extracts (reviewed by Hirano, 1999). Analysis of molecules like Mcd1/Scc1p (related to Rad21p), Scc3p, Smc1p, and Smc3p, currently proposed as cohesion proteins per se (Guacci et al., 1997; Michaelis et al., 1997; Toth et al., 1999 and references therein), showed that sister chromatid cohesion is functionally related to other aspects of chromosome metabolism. The *mcd1* mutant is also defective in chromosome compaction (Guacci et al., 1997), and several cohesion mutants display hypersensitivity to DNA-damaging agents, suggesting a link between chromosome structure and DNA repair (review in Hirano, 1999).

Genetic and cytogenetic analyses have also been powerful tools for dissection of meiotic chromosome morphogenesis (e.g., Moore and Orr-Weaver, 1998). All known mutants defective in meiotic chromatid cohesion exhibit premature loss of sister centromeric connections during meiosis I with subsequent abnormal chromosome segregation. The *Drosophila meiS322* mutant appears specifically defective in maintaining centric connections at meiosis I (e.g., Tang et al., 1998). Other mutants (e.g., *Sordaria spo76-1*, fission yeast *rec8*, and budding yeast *red1*) exhibit, additionally, cohesion defects along the arms as early as prophase plus defects in AEs (Moreau et al., 1985; Molnar et al., 1995; Smith and Roeder, 1997; Bailis and Roeder, 1998). The maize *dy1* and *dsy1* mutants make SCs but lose sister cohesion during the pachytene-to-diplotene transition (Maguire

‡ To whom correspondence should be addressed (e-mail: zickler@ igmors.u-psud.fr).
§ Present address: Department of Genetics, Agricultural University, Dreijenlaan 2, 6703 HA Wageningen, The Netherlands.

et al., 1993). Finally, the *Drosophila ord* mutant exhibits early prophase defects and absence of sister cohesion prior to metaphase I (Bickel et al., 1997). Correspondingly, MEI-S332 protein localizes to centromere regions from prometaphase I to anaphase II (Moore et al., 1998), while Red1p localizes along chromosomes throughout prophase (Smith and Roeder, 1997). Notably, except for *meiS322*, these mutants are also defective in meiotic recombination, suggesting that critical aspects of meiotic interhomolog interactions are functionally related to the intersister interaction process (e.g., Kleckner, 1996; Roeder, 1997).

To shed light on the relationships among these diverse processes, we have further analyzed the roles of the *Sordaria SPO76* gene. Previous studies have shown that the *spo76-1* mutant is defective in meiotic sister chromatid cohesion and mitotic DNA repair (Moreau et al., 1985; Huynh et al., 1986). Here, we report cloning of *SPO76*, Spo76p localization throughout mitosis and meiosis, and further analysis of *spo76-1* phenotypes. Such analysis is facilitated by the fact that *Sordaria* chromosomes are large enough to be directly visualized in all stages of both programs. Spo76p is an evolutionarily conserved protein with homologs in fungi and in human. Spo76p is chromosome associated in both mitosis and meiosis except at metaphase(s) and anaphase(s). During meiotic prophase, Spo76p is mostly axis associated. A specific *spo76-1* defect occurs at mitotic prometaphase, with cohesion and compaction coordinately affected on a regional basis. This phenotype points to the existence of a critical chromosomal transition point, corresponding to the onset of higher order chromosome compaction, where cohesion and chromosome condensation are functionally linked and where Spo76p plays a crucial role. The meiotic defects of *spo76-1* can be explained analogously, with the addition of a program-specific difference that correlates with meiosis-specific features of Spo76p chromosome localization. These and other results suggest that Spo76p is a conserved component of basic chromosome structure that has been recruited from the mitotic cycle and functionally adapted for use in the meiotic program.

## Results

### Spo76p Is Evolutionarily Conserved from Fungi to Human
The *SPO76* gene was cloned from a *Sordaria macrospora* genomic cosmid library by transformation and SIB selection (Akins and Lambowitz, 1985). The *SPO76* gene was mapped to the only major open reading frame (ORF) present on a complementing 6.4 kb PstI-SmaI fragment by the strategy of Turcq et al. (1990). The *SPO76* ORF comprises 4791 bp, interrupted by two small introns (of 62 bp and 73 bp), whose presence was confirmed by sequencing of corresponding cDNAs. To verify that we had cloned the *SPO76* gene and not a suppressor, the *spo76-1* allele and the wild-type allele from the isogenic parent strain were also sequenced. The *spo76-1* allele differs from the isogenic wild-type by two deletions: a 1 bp deletion causes a frameshift, but the reading frame is subsequently restored by the second deletion of 11 bp. The two mutations together
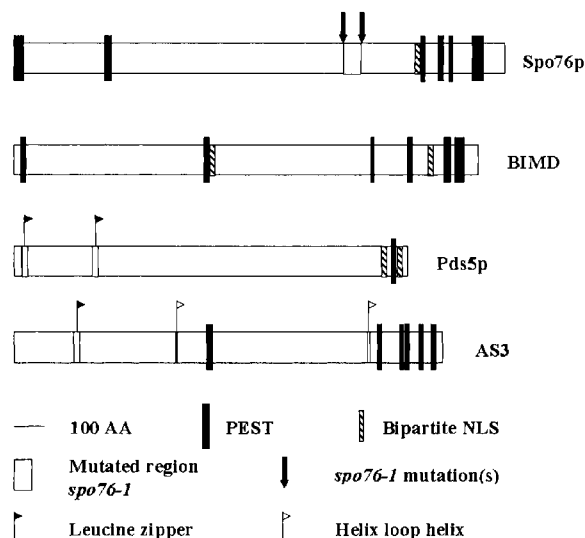


Figure 1. Spo76p and Its Three Cognate Proteins
For sequence alignments, see the website <http://www.cell.com/cgi/content/full/98/2/261/DC1>.

change a region of 60 aa in the Spo76 protein (Figure 1). *spo76-1* is unlikely to be a null allele (see Discussion).

The *SPO76* ORF encodes a potential protein of 1579 amino acids (aa) with a predicted molecular mass of 176.9 kDa and an average pI of 5.4. Database searches plus evaluation of the quality of alignment expressed by the Z parameter (Slonimsky and Brouillet, 1993) show that the predicted Spo76p shares significant homology with three proteins and the putative products encoded by two cDNA fragments. The three proteins are BIMD of *Aspergillus nidulans* (Denison et al., 1992), Pds5p of *Saccharomyces cerevisiae* (accession Q04264), and an androgen-induced prostate proliferative shutoff-associated protein encoded by the human *AS3* gene (Geck et al., 1999). Percentages of identity are, respectively, 44%, 30%, and 22%; Z scores are 84, 38, and 24. The two incomplete proteins are a 390 aa fragment from *Schizosaccharomyces pombe* (accession AF049529) and an 851 aa fragment of the human KIAA0648 protein (accession AB014548), with percentages of identity of 32% and 23% and Z scores of 31 and 18. Notable features of the four complete proteins (Figure 1) include numerous potential PEST sequences, proposed to target proteins for proteolysis (Rechsteiner and Rogers, 1996); bipartite nuclear localization signals (bipartite NLS in Spo76p, BIMD, and Pds5p); and putative DNA-binding motifs (leucine zipper in Pds5p and AS3; helix loop helix in AS3).

### Spo76p Localizes to Foci on Chromosomes at All Stages of the Mitotic Cycle Except Metaphase and Anaphase
The cytological localization of Spo76p was determined using epitope- and reporter-tagged versions of the protein, carrying carboxy-terminal additions of, respectively, a triple hemagglutinin (HA) epitope and green fluorescent protein (GFP). Each construct, when introduced into a *spo76-1* strain, complemented the *spo76-1* meiotic and sporulation defects with exactly the same
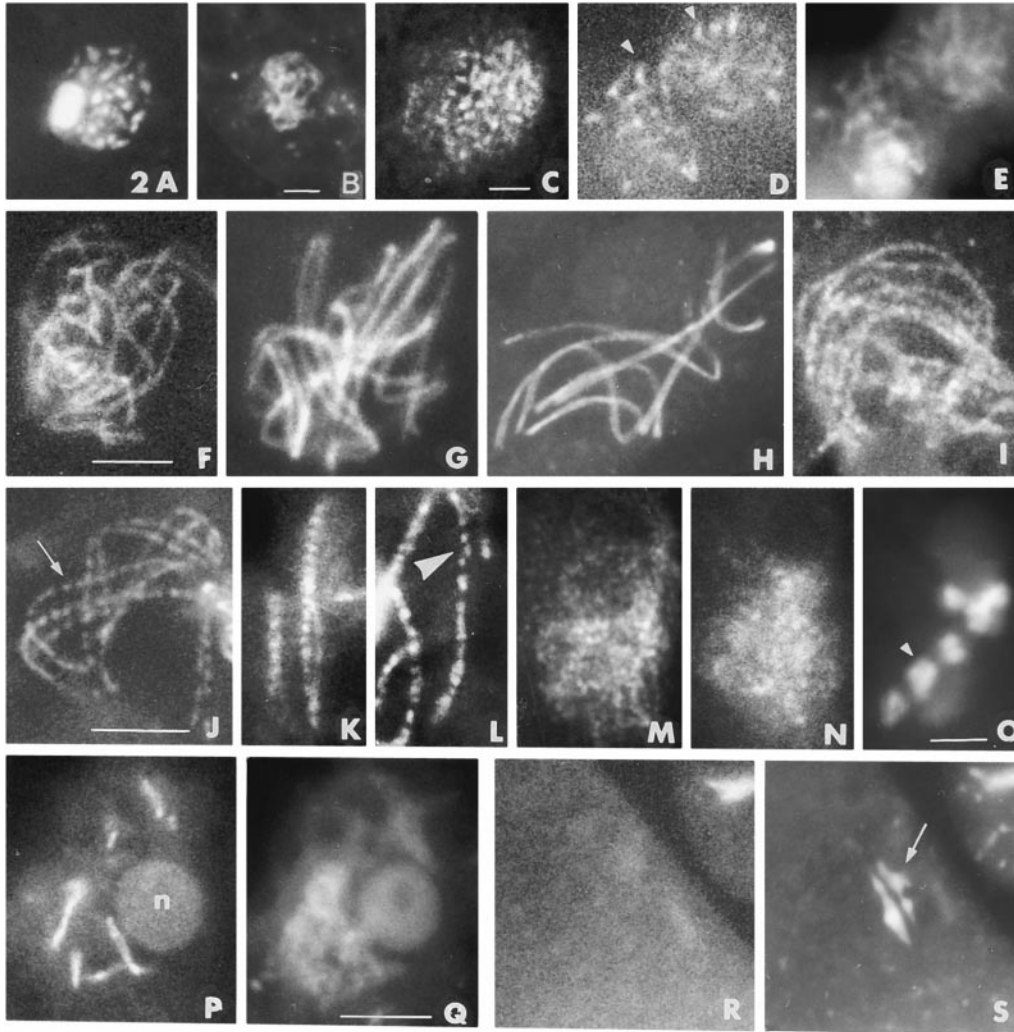
Figure 2. Spo76p Localization during Mitosis and Meiosis

(A–C) Mitotic prophase nuclei stained with (A) Spo76-GFPp (the nucleolus is visible left of the foci) and (B) corresponding DAPI; (C) Spo76-HAp. (D–S) Meiosis. (D) Karyogamy nucleus with short Spo76-GFPp lines at chromosome ends (arrowheads). (E) Corresponding DAPI. Spo76-GFPp stains as continuous lines along the chromosomes of leptotene (F), early zygotene (G), and pachytene (H) nuclei. (I–O) Nuclei stained with Spo76-HAp. (I) Leptotene. (J) Spread early zygotene; the arrow points to homologous nonsynapsed regions. Pachytene bivalents show clear punctuate pattern with either matching (K) or in staggered (L) rows of spots (indicated by the arrowhead). (M) Diffuse stage. (N) Diplotene with corresponding (O) DAPI (arrowhead points to one of the seven bivalents). (P) Spo76-GFPp in diffuse stage and corresponding DAPI (Q) at corresponding focus level. (R) Metaphase I and corresponding DAPI (S) with arrow indicating three bivalents. Bars, 5 μm.

efficiency as the 6.4 kb complementing subclone: the average number of complemented transformants per transformation (4 in total) was 10.5 for -HA, 9.8 for -GFP and 9.5 for the 6.4 kb subclone.

Spo76p staining is exclusively observed in nuclei. Spo76p localizes as foci in nuclei of all mitotic stages except metaphase and anaphase. The disappearance of Spo76p at prometaphase precedes any discernible separation of sisters (the metaphase/anaphase transition). Foci are best defined in nuclei from cells of the sexual cycle, which are larger (Figures 2A and 2B). Such nuclei exhibited ~27 Spo76-GFPp foci (range 19–36 among 100 nuclei representing all relevant cell cycle stages). Foci were usually seen located along the chromosomes, but in nondividing nuclei they sometimes also occurred outside of the main chromosome area. Spo76-HAp gave the same results except that foci were both smaller and more numerous (range 40–70; compare Figures 2C and 2A). In all cases, foci were much brighter in telophase and prophase nuclei than in interphase nuclei.

## Spo76p Localizes along Meiotic Chromosomes as Foci at Early and Late Prophase and as Lines at Midprophase

By both approaches, meiotic prophase nuclei are more brightly stained than any other nuclei of either vegetative or sexual cycles. Meiotic stages can be defined independently of chromosome status by three criteria: the ascus length, which increases 10-fold from leptotene to metaphase I; the nucleolar shape and localization when compared to the chromosome mass; and the nuclear volume, which increases progressively (5-fold) during prophase.

Before karyogamy, Spo76-GFPp is observed in foci. Concomitant with nuclear fusion, these foci become organized into short lines, a change that initiates preferentially at the chromosome ends (Figures 2D and 2E). Thereafter, Spo76-GFPp stains as continuous lines along the lengths of all unsynapsed (leptotene), synapsing (zygotene), and synapsed (pachytene) chromosomes (Figures 2F–2H).

Spo76-HAp exhibits this same staining pattern except that finer details can be seen. At early leptotene, each chromosome has a single continuous line of regularly spaced dots plus some fainter foci in what we infer to be the peripheral chromatin (Figure 2I). From late leptotene to midpachytene, continuous lines are observed, though vigorously spread chromosomes exhibit contiguous regularly sized dots at these stages as well (illustrated for early zygotene in Figure 2J). At late pachytene, however, a punctuate pattern of staining is always seen, with linear rows of dots ($2.07 \pm 0.2$ foci per $\mu$m along 50 bivalents) that are more prominent and less regular in spacing and size than earlier (Figures 2K and 2L). Interestingly, foci on homologs do not always occur at matching positions (arrowhead in Figure 2L).

Spo76p was shed from the bivalents at diplotene by both approaches, but with slightly different patterns. For Spo76-HAp, the bright pachytene punctuate pattern (Figure 2L) is rapidly lost when cells enter the diffuse stage preceding diplotene (Figure 2M), and diplotene nuclei contain only small foci spread over the entire chromatin mass (Figures 2N and 2O). For Spo76-GFPp, in contrast, early diffuse-stage nuclei still contain seven bright lines, but these are no longer axes associated, as deduced from the fact that they are seen in a different focal plane from the chromatin mass of the bivalents (Figures 2P and 2Q). These lines subsequently break into smaller spots until, finally, GFP fluorescence is lost after middiplotene. With respect to external staging criteria (above), assembly and disassembly of Spo76p into and out of linear arrays during meiotic prophase I correspond closely to the formation and disassembly of AEs. Furthermore, the earliest segments of AE, like the earliest linear arrays of Spo76p foci, tend to occur at chromosome ends. Finally, by both approaches, Spo76p is not detected on metaphases or anaphases I (Figures 2R and 2S) and II but reappears along chromosomes as foci at telophase I, prophase II, and telophase II. Thus, as during mitosis, Spo76p is seen on meiotic chromosomes at all stages except metaphase(s) and anaphase(s).

Overall, the two tagged Spo76p give similar staining patterns, though Spo76-GFPp tends to give more uniform or continuous staining than Spo76-HAp. While we cannot exclude a true difference between the two situations, it is equally possible that the underlying distribution of Spo76p is the same for both versions of the protein. Regions of greater abundance may alternate with regions of lesser abundance, with peculiarities of the two detection systems accentuating or minimizing this variation. For example, the Spo76-HAp signal might be attenuated in regions of lower protein abundance due to absence of specific epitopes. Oppositely, the Spo76-GFPp fluorescence might give a strong signal at low protein level but saturate at high protein level to give an apparently smoother distribution.

The SPO76 GFP-tagged sequence exhibited the same
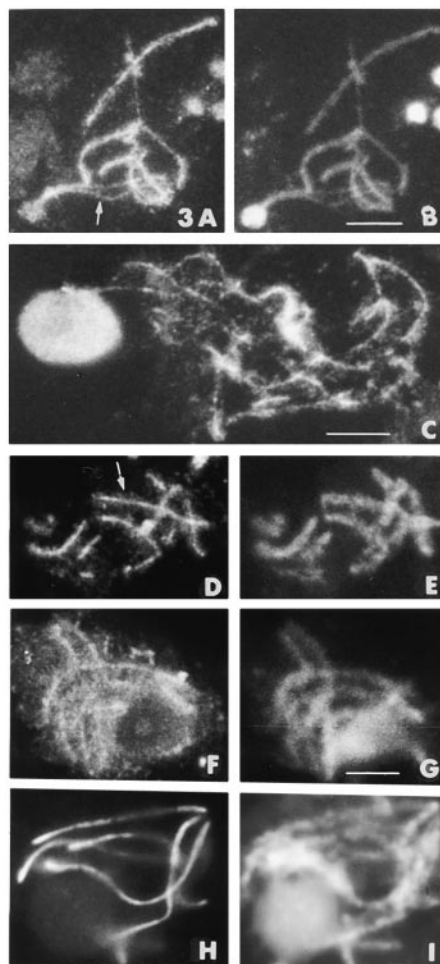


Figure 3. MPM-2 Staining of Meiotic Prophase Nuclei

(A) Spread wild-type late zygotene; arrow points to two synapsing homologs. (B) Corresponding DAPI. Lines of fine dots seen along each chromosome are similar in wild type (A) and spo76-1 (C) zygotene nuclei; the nucleolus is stained in both strains. (D) Pachytene wild-type nucleus with faint chromatin staining (arrow); MPM-2 signal is clearly narrower than the DAPI staining (E). Double-stained pachytene nucleus with MPM-2 antibody (F) and Spo76-GFPp (G). The GFP signal is less bright than in (H) due to the longer fixation needed for the double labeling. Spo76-GFPp pachytene nucleus (H) and corresponding DAPI (I). Bars, 5 $\mu$m.

staining pattern of both the mitotic and meiotic nuclei when present in a wild-type strain background as when present in a spo76-1 background (data not shown). Thus, protein localization is not affected by the presence of the mutant protein or by an extra amount of wild-type protein.

## MPM-2 Defines a Narrower Staining Pattern along Meiotic Chromosomes Than Does Spo76p

The monoclonal phosphoprotein antibody MPM-2 (Davies et al., 1983) recognizes topoisomerase II$\alpha$ in mitotic chromosome scaffolds (e.g., Taagepera et al., 1993). In Sordaria, this antibody stains the chromosomal axes during meiotic prophase (Figures 3A and 3B). Rows of discrete and almost contiguous foci are seen along the lengths of leptotene, zygotene, and early pachytene
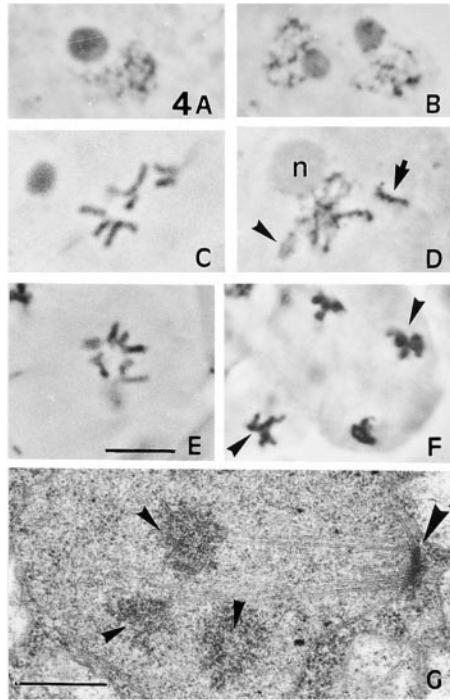
Figure 4. Mitotic Phenotypes

(A–F) Hematoxylin-stained mitotic nuclei (LM). Protoplast wild-type (A) and *spo76-1* (B) prophase nuclei. (C) Wild-type prometaphase. (D) Chromosome arms with either discernibly separated (arrowhead) or conjoined kinky chromatids (arrow) in an early *spo76-1* prometaphase nucleus. (E–G) *spo76-1*. (E) Metaphase. (F) Two synchronous anaphases (arrowheads). (G) Electron micrograph of a metaphase spindle; small arrowheads indicate chromosomes; large arrowhead points to the SPB. n, nucleolus. Bars, 5 $\mu$m (LM) and 0.5 $\mu$m (EM).

chromosomes in both wild type (Figure 3A) and *spo76-1* (Figure 3C). The MPM-2 signal is much narrower than the DAPI signal at all times and, at pachytene, forms a single line running down the middle of the bivalent (Figures 3D and 3E). However, some peripheral chromatin staining can be observed, for example, as tiny, faint foci in a halo around the axial signal (e.g., arrow in Figure 3D). Staining is no longer detectable after pachytene.

MPM-2 and Spo76p staining (above) are contemporaneous. Interestingly, the MPM-2 signal is narrower than the Spo76-GFPp signal (Figures 3F and 3G). In fully synapsed bivalents, the Spo76-GFPp lines define a narrower region of each bivalent than that of DAPI-stained chromatin, implying preferential localization of Spo76p in the vicinity of the chromosome axes (Figures 3H and 3I). Thus, while both signals are axis associated, the MPM-2 epitopes appear to be more tightly localized to the bases of the chromatin loops than is Spo76p. This result suggests that Spo76p may establish sister cohesion in relationship with, but immediately above, the AEs (i.e., in a "supraaxial" position).

### *spo76-1* Exhibits Defective Mitotic Chromosome Morphogenesis at Prometaphase but Not at Later Stages

The effect of *spo76-1* on mitosis was examined by light and electron microscopy. Prophase was normal (compare Figures 4A and 4B), but striking effects of the *spo76-1* mutation were seen at prometaphase. First, while prometaphase nuclei are rare in wild-type mycelia and protoplasts (5/100 nuclei), they were frequently observed in *spo76-1* (60/100), implying prolongation of this stage in the mutant. Second, mutant chromosome morphology and morphogenesis are significantly altered. In wild-type mitoses, chromosome compaction proceeds smoothly from modest chromosome individuality at prophase to a fully compacted metaphase condition; moreover, sister chromatids are never discernibly distinct (Figure 4C) until anaphase. In *spo76-1* prometaphases, in contrast, (a) chromosomes exhibit segments in which sister chromatids are distinctly separated from one another (arrowhead in Figure 4D); (b) chromatin has a markedly fuzzy appearance (compare Figures 4D and 4C); (c) chromosomes are longer than normal for this stage; and (d) some chromosome segments or arms exhibit a kinky appearance, indicative of higher order coiling/folding (arrow in Figure 4D), again a morphology never observed in the 100 analyzed wild-type nuclei. Interestingly, the sister chromatid cohesion and the axial compaction phenotypes vary in concert along the chromosome arms (Figure 4D; Discussion).

However, despite these differences at prometaphase, mutant and wild-type nuclei are essentially indistinguishable at later stages. During the metaphase/anaphase transition, *spo76-1* chromosomes are as compact as wild-type chromosomes, and sisters are no longer separated (Figure 4E). Furthermore, chromosome segregation at anaphase (Figure 4F) is qualitatively normal. First, *spo76-1* protoplasts examined at regular intervals for 24 hr after their preparation do not produce dead cells, and their nuclei exhibit the same size—both strong indications that chromosome segregation is regular (absence of aneuploidy). Second, anti-tubulin immunofluorescence revealed that mitotic spindles showed no gross abnormalities. Third, electron microscopy confirmed that *spo76-1* chromosomes, microtubules, and SPBs were similar to wild type, at least in premeiotic mitoses (Figure 4G). Finally, despite a prometaphase pause, *spo76-1* exhibits an essentially normal growth rate at a wide range of temperatures (13°C, 23°C, 30°C, and 34°C).

### *spo76-1* Exhibits Axial Element Splitting plus Coordinate Absence of Synaptonemal Complex Formation

The ultrastructural hallmark phenotype of the *spo76-1* mutant was splitting and discontinuity of AEs at midprophase (Moreau et al., 1985). Serial reconstructions of 20 prophase nuclei, nine available from previous work and eleven more made for the current study, revealed additional *spo76-1* defects. In wild type, AEs are formed as small stretches just after karyogamy and are complete at leptotene for all chromosomes. The same is true for *spo76-1* except that AEs were clearly less dense and more irregular in shape than in wild type (compare Figures 5A and 5B). Since wild-type AEs are less regular at early than at late leptotene, the *spo76-1* mutation may "exaggerate" these early phenotypes.

Wild-type zygotene and pachytene nuclei always show, respectively, seven synapsing and regularly synapsed SCs. Mutant nuclei, in contrast, were all abnormal, in several respects. Most AEs showed split segments, with all split AEs being half as wide as unsplit
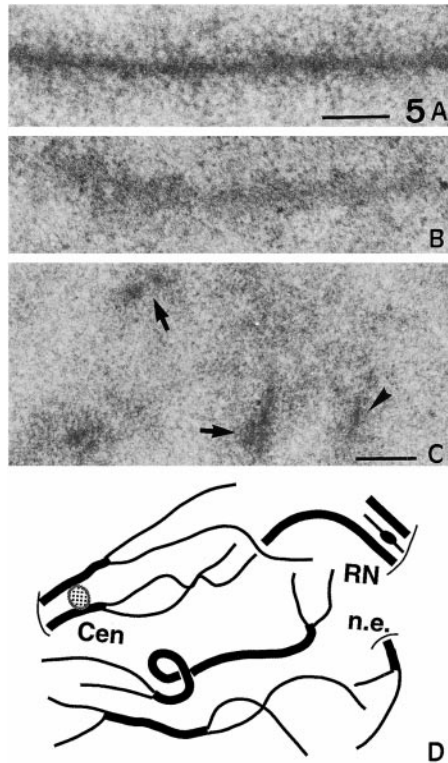
Figure 5. Electron Micrographs of Sectioned AEs

AEs from (A) wild-type and (B) *spo76-1* leptotene nuclei. (C) Section in a *spo76-1* nucleus showing both split AEs (arrows) and a half AE (arrowhead). (D) Reconstruction of four *spo76-1* chromosomes illustrative of the different mutant phenotypes; thick lines indicate unsplit AEs and thin lines, split AEs. Cen, centromere; RN, recombination nodule; n.e., nuclear envelope. Bars, 0.5 μm.

ones (arrowhead in Figure 5C). Overall, few AEs could be followed from telomere to telomere because split regions, whose two "half AEs" extended widely from one another (Figure 5D), were often broken. The total AE length (split plus unsplit) per nucleus was, however, approximately normal (79–86 μm versus 86–96 μm in wild type), suggesting that discontinuities reflect primarily breaking, rather than disassembly of AE components. Nuclei contained only 2–11 SC pieces per nucleus, representing 10% of the wild-type SC length. Interestingly, split AE and SC morphologies varied coordinately along the chromosomes; when SC was present, AEs were intact, and in regions with split AEs, SCs were absent, though a few segments exhibited unsynapsed but unsplit AEs. Also, virtually all centromeric regions (identifiable as fuzzy densities irrespective of AE/SC status) remained connected by a piece of SC or two intact AEs (Figure 5D).

### *spo76-1* Exhibits Diffuse, Kinked, and Partially Split Chromosomes at Meiotic Midprophase plus Full Sister Separation and Delayed Chromosome Compaction at Diplotene/Prometaphase

A striking feature of *spo76-1* meiosis is that, by LM, 28 chromosomes are regularly observed at metaphase I rather than the 7 bivalents seen in wild type (n = 7),

implying that sister chromatids fully separate prematurely (Moreau et al., 1985). To understand this phenotype, we performed a detailed LM study of *spo76-1* meiosis.

The mutant shows normal fruiting-body development, implying that premeiotic stages including karyogamy are occurring normally. In wild-type prophase, chromosomes are straight and clearly individualized from leptotene (Figure 6A) through pachytene (Figures 6B and 6C). The corresponding *spo76-1* nuclei, in contrast, showed mainly kinky and diffuse chromosomes (compare respectively Figures 6D, 6E, and 6F). The presence of kinkiness (arrowheads in Figures 6D and 6E) implies some tendency for folding/coiling of mutant chromosomes, a feature never observed during wild-type meiotic prophase (Figures 6A–6C). In addition, *spo76-1* chromosomes exhibited coordinate regional defects in sister cohesion and homologous synapsis from late leptotene onward (e.g., arrows in Figure 6F; Discussion). Thus, the AE and SC defects are also reflected at the level of bulk chromatin.

Wild-type chromosomes exit pachytene into the diffuse stage, where chromosome individualization is lost, and then reemerge into diplotene, where sister chromatids are closely juxtaposed but homologs are separated except at chiasmata. While the diffuse stage was grossly similar in both strains (Figures 6G and 6H), the onset of diplotene in the mutant showed important differences. In wild-type nuclei, chromatin condenses progressively, and all bivalents show chiasmata (Figure 6I). In *spo76-1*, chromosomes come out of the diffuse stage less compacted than in wild type (compare Figure 6J with 6I). Furthermore, when diplotene condensation starts, 28 chromosomes emerge (Figure 6K and compare with 6L). Since the mutant still exhibited seven bivalents at pachytene, albeit with a tendency for sister splitting, additional loss of cohesion must occur specifically during the diffuse stage–diplotene transition.

At prometaphase and metaphase I, the final degree of chromosome compaction (Figures 6K and 6L) and spindle formation (Figures 6M and 6N) is similar in both strains. At anaphase I, the 28 chromosomes of the mutant segregate randomly on an elongated spindle (Figure 6N). The mutant also undergoes a cell cycle arrest at this stage: 2-week-old asci still exhibit elongated spindles, whereas wild-type asci form eight ascospores after 4 days. Presumably, since individualized sister chromatids cannot undergo bipolar alignment, absence of tension activates the spindle attachment checkpoint (see Nicklas et al., 1995). Only 1%–5% of the asci go through meiotic second division, and even fewer form ascospores. None of the 200 tested ascospores ever germinated (versus 99% germination in wild type).

### *spo76-1* Is More Defective for Late Recombination Nodules Than for Formation of Dmc1p and Rad51p Foci

Since a *spo76-1* homozygote produces no viable ascospores, recombination levels cannot be measured. Moreover, since chromatid cohesion is lost before diplotene, recombination cannot be evaluated by counting chiasmata. A role for *SPO76* in recombination can, however, be inferred by analyzing recombination nodules. In *Sordaria*, as in other organisms, SC-associated late
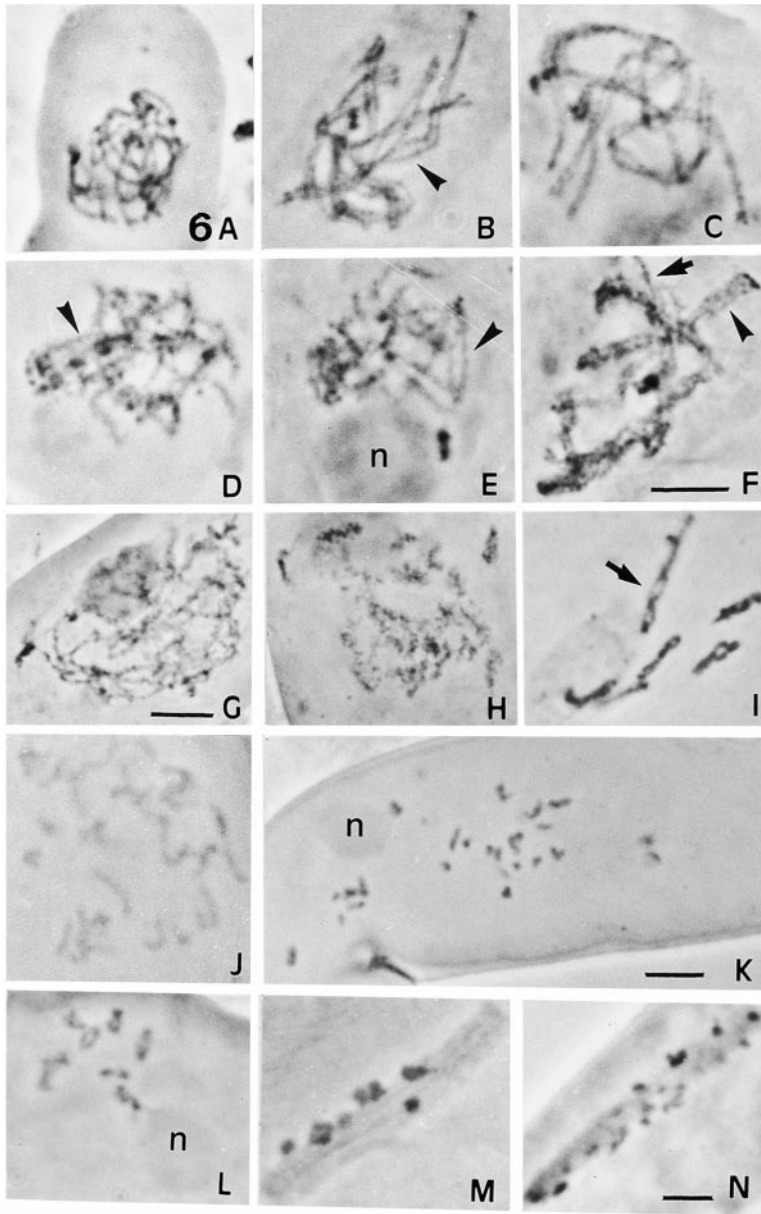
Figure 6. Meiotic Phenotypes

Wild-type leptotene (A), zygotene (B), and pachytene (C) nuclei. The *spo76-1* chromosomes are kinky (arrowheads) in all leptotene (D) and zygotene (E) nuclei. (F) Mutant pachytene nucleus in which chromosome regions show either widely (arrow) or slightly (arrowhead) separated chromatid regions. Wild-type (G) and mutant (H) diffuse stage. (I) Wild-type diplotene nucleus with clear chiasmata (arrow). (J) Mutant diplotene. Although mutant chromatids are separated (K), condensation is similar in mutant (K) and wild-type (L) prometaphase chromosomes. Wild-type (M) and mutant (N) metaphases I. n, nucleolus. All nuclei are stained by hematoxylin. Bars, 5 μm.

recombination nodules (LNs) correspond to crossovers (Zickler et al., 1992). The mean number of LNs (Figure 7A) in homozygous *spo76-1* is about one-sixth the wild-type level: 4.1 (range 2–6 in 16 pachytene nuclei) versus ~25 (range 23–26 in 100 pachytene nuclei) in wild type, suggestive of a reduction in crossovers. Since mutant SCs are discontinuous, one cannot rule out that additional LNs might occur in regions lacking SCs, but the reliability of the LN findings is further supported by the fact that the +/*spo76-1* heterozygote, which has normal SCs, exhibits a ~40% reduction in both LNs and crossovers (Zickler et al., 1992).

In yeast, where most or all meiotic recombination events are initiated by meiosis-specific double-strand breaks (DSBs), immunostaining foci of Dmc1p and Rad51p appear only when DSBs have occurred (e.g., Bishop, 1994). Thus, analysis of Dmc1p or Rad51p foci should provide insight into the efficiency with which

meiotic recombination is initiated. In wild-type *Sordaria* nuclei, as in yeast, each of the two antibodies localized to foci only on leptotene and early zygotene chromosomes (Figures 7B and 7C), with ~25–35 foci per nucleus (50 analyzed). Precise counting of foci along each bivalent is impossible, as spreading of nuclei at these stages is difficult.

In homozygote *spo76-1* nuclei (Figures 7D and 7E), a 30% reduction was observed in the number of Dmc1p and Rad51p foci (18–24 in 50 leptotene/early zygotene nuclei). Also, contrary to wild type, all mutant nuclei (50 observed) showed 3–8 bright Rad51p foci at early pachytene (according to external staging criteria). The high level of Rad51/Dmc1p foci in *spo76-1* suggests that recombination initiation is nearly normal. The contrast with the low level of LNs suggests a strong defect specifically in the later stages of recombination, at least for events associated with crossovers.
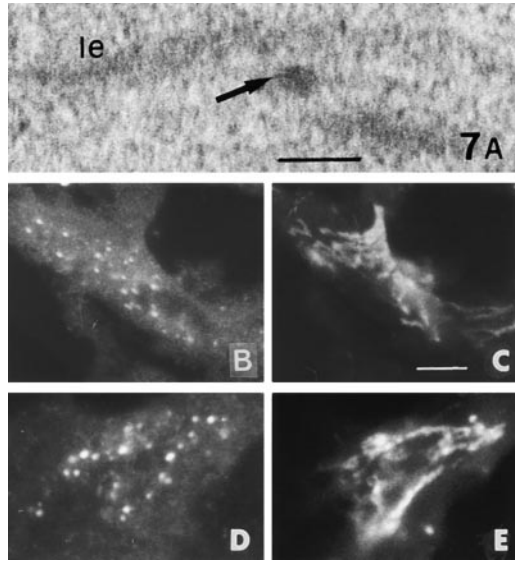
**Figure 7. LN and Rad51p Localization**

(A) Electron micrograph of a mutant SC piece with associated LN (arrow). Rad51p foci in squashed early zygotene wild-type (B) and mutant (D) nuclei and their corresponding DAPI (C and D). Bars, 0.5 μm in (A) and 5 μm in (B–E).

## Discussion

### Spo76p Is a Conserved Chromosome Morphogenesis Protein

Spo76p is evolutionarily conserved from yeast to human. Fungal homologs are BIMD (*A. nidulans*) and Pds5p (*S. cerevisiae*). The *Sordaria SPO76* gene can complement the temperature-sensitive lethality conferred by a *bimD6* mutation (D. v. H., unpublished results), implying direct functional homology between the cognate proteins. Accordingly, existing mutants of *SPO76*, *BIMD*, and *PDS5* show interrelated defects in chromosome morphogenesis during the mitotic cycle. The *spo76-1* mutant is defective in sister chromatid cohesiveness and chromosome compaction at prometaphase and is hypersensitive to DNA damage (above). At nonpermissive temperature, the *bimD* mutants show random chromosome localization along the spindle and anaphase arrest, phenotypes consistent with a cohesion defect; at permissive temperature they exhibit DNA damage hypersensitivity (Denison et al., 1992). The *pds5* mutant exhibits precocious dissociation of sister chromatids (SGDID S0004681). Since *BIMD* is an essential gene (Denison et al., 1992), the same is likely true of *SPO76*, with *spo76-1* being a specialized, non-null allele.

Interestingly, Spo76p is also significantly homologous to the products encoded by two human sequences. Since the *BIMD* gene occurs as a single copy in the *Aspergillus* genome (Denison et al., 1992), a gene duplication might have occurred during evolution, possibly with concomitant functional specialization of the two genes. Two facts suggest that *SPO76*, while required for both mitotic and meiotic divisions, may also play a crucial role during the G1-S interval. First, Spo76p is present in all nondividing nuclei. Second, overexpression of the *BIMD* gene is lethal because it blocks cells in the G1-S interval (Denison et al., 1992). The fact that proliferative shutoff of human prostate cells requires the androgen-induced expression of the *AS3* gene (one of the two potential human homologs of *SPO76*) (Geck et al., 1999) could be explained analogously; in this case, hormone-induced (over)expression of AS3p might prevent entry into mitosis. It would also be interesting to know whether the two roles of the fungal protein, in the divisions and at G1-S, might be implemented by the two different human Spo76 homologs.

Spo76p is unrelated in sequence to any of the known yeast or *Xenopus* cohesins (review in Hirano, 1999). Interestingly, however, the conditional lethal phenotype conferred by the *bimD6* mutation can be suppressed by a mutation in the gene encoding SUDA, the *Aspergillus* homolog of the cohesin protein Smc3p (Holt and May, 1996). Furthermore, the timing of Spo76p localization is similar to that observed for *Xenopus* cohesins, which also are depleted from chromosomes at or before metaphase (Losada et al, 1998). Thus, the possibility remains open that Spo76p is an additional member of the cohesins complex. In any case, while one cannot exclude very low levels of Spo76p remaining on chromosomes, particularly since it reappears at telophase, the timing of Spo76p localization points to roles other than maintenance of sister cohesion at the metaphase/anaphase transition.

Spo76p is also required for normal meiotic chromosome morphogenesis. The *spo76-1* mutation confers pronounced defects in intersister cohesion and chromosome compaction during prophase. Those defects are closely related, but not identical, to those seen at mitotic prometaphase. Meiotic recombination is also defective. Meiotic phenotypes of *pds5* have not been reported, but *bimD* mutants are sterile (D. v. H., unpublished results). Spo76p is found associated with chromosomes in the meiotic program similarly as during the mitotic program except for increased continuity at meiotic prophase, a difference concordant with meiosis-specific aspects of this period. These findings (below) suggest that Spo76p is a component of basic chromosome structure recruited and functionally adapted for the meiotic program.

### A Critical Role for Spo76p at the Transition from Prophase to Prometaphase in the Mitotic Cycle

The *spo76-1* chromosomes are morphologically normal at all stages of the mitotic cycle except at prometaphase. This stage corresponds to the transition between the extended prophase chromosome configuration and the more compact metaphase configuration. The *spo76-1* phenotype fits with the notion that the onset of higher order compaction represents a discrete transition point in chromosome morphogenesis, in which Spo76p may play a critical role. Interestingly, also, mutant nuclei accumulate at the point of the defect, implying that exit from prometaphase is delayed for structural and/or regulatory reasons.

The prometaphase mutant phenotype includes defects in sister chromatid cohesion, axial shortening, and chromatin compactness, which points to functional coordination among these three different aspects of chromosome morphogenesis. A mutant situation in which

sister cohesion and chromosome compaction are coordinately disrupted was first described for yeast *mcd1* (Guacci et al., 1997). Interestingly, the *spo76-1* defects vary in concert, from region to region along the chromosome arms: a split and loose morphology alternates with a conjoined and tight morphology that includes pronounced kinking. This pattern provides strong evidence that the three different aspects of chromosome morphology not only involve common components but are directly coupled at the mechanistic level. A similar situation has also been observed for Indian muntjack mitotic chromosomes (Gimenez-Abian et al., 1995). In that system, prometaphase corresponds to a transition between prophase chromosomes having a single conjoined linear core (silver stained) and metaphase/anaphase chromosomes having two cores that are split and kinked. Chromosomes progress through intermediate morphologies, and the first of these is essentially identical to the *spo76-1* prometaphase: along the chromosomes, regions of conjoined kinked cores alternate with regions of straight, less well-defined, and separated cores.

On the basis of these data, we could suggest that the prophase to metaphase transition involves the imposition of special forces on the chromosomes as required for initiation of higher order compaction and that Spo76p is required for chomosome integrity during this transition, as part of the force transduction mechanism. In *spo76-1*, the force or stress is imposed normally but then relieved, on a region by region basis, either by loss of both cohesion and chromatin compactness or by a relatively normal process in which cohesion and compactness are maintained and axial coiling/folding occurs but in an attenuated form. The presence of Spo76p on prometaphase chromosomes, but not at metaphase, would further suggest that Spo76p normally leaves the chromosomes either concomitant with, or as a consequence of, these events.

### Critical Roles for Spo76p during Recombination and at Two Transition Points during Meiosis

A strong meiotic defect in *spo76-1* chromosome morphogenesis is first observed at late leptotene, after AEs are fully formed. This defect includes general chromosome diffuseness plus splitting of AEs. Since nuclei can be found in which splitting of AEs (EM) or bulk sister chromatin (LM) have occurred in the absence of SC formation (EM) or homologous synapsis (LM), AE splitting appears to precede SC formation (i.e., zygotene).

The fact that SC forms only in regions of unsplit AEs could reflect an intrinsic inability of SC to form between "half AEs." SCs can, however, form perfectly normally in such a situation: in the *Coprinus* mutant *spo22*, which skips premeiotic S phase, single chromatids form AEs and these "half AEs" synapse into regular SCs (Pukkila et al., 1995). Thus, we favor the alternative interpretation for *spo76-1* that AE splitting and formation of SCs with unsplit AEs comprise two alternative responses, implemented on a region-by-region basis, to a single underlying problem that arises at the leptotene/zygotene transition.

The meiotic midprophase *spo76-1* phenotype is strikingly similar to the mitotic prometaphase phenotype. Both include chromosomal diffuseness; each involves a prominent defect at a specific transitional stage; and in both cases, chromosome arms exhibit a binary response in which some regions exhibit split sisters and a less ordered conformation, while other regions exhibit unsplit sisters and a more ordered conformation. Indeed, in a precise analogy, wide separation of split AEs could imply local chromatin bulkiness, which precludes intimate juxtaposition of nonsister axes into the SC, while unsplit regions might have more compact chromatin and thus be able to make SCs. Also, in both cases, centromeres remain largely unaffected. It is therefore tempting to envision that meiotic leptotene/zygotene transition is, in fact, the meiotic equivalent of the mitotic prophase/prometaphase transition, with Spo76p playing analogous roles in both situations.

There is, however, one obvious difference between the two transition points: the mitotic prophase/prometaphase transition signals the onset of higher order chromosome folding/coiling, while during meiosis this phase does occur much later, after the diffuse stage. This difference can be explained by saying that the same triggering chromosomal transition occurs in both cases but in meiotic midprophase does not provoke chromosome coiling/folding due to the extra stiffness/resistance from the chromosomes, which have structurally prominent, very straight axes (AEs) as compared to their mitotic prophase counterparts. Such a scenario is supported directly by the fact that *spo76-1* exhibits chromosome kinking from late leptotene through pachytene. This finding implies that some sort of force for axial compaction is exerted at the appropriate stage and, moreover, that Spo76p is required for the normal block to such compaction. Furthermore, the fact that Spo76p exhibits more continuous staining along the chromosome axes during meiotic than during mitotic prophase provides a direct structural correlate for such a meiosis-specific role. In further support of the occurrence of a disruptive force as a normal feature of leptotene/zygotene, there is also clear evidence for a tendency for individualization of sister chromatids at this transition in other organisms as exemplified by 3D analyses of maize meiosis (Dawe et al., 1994 and references therein).

The *spo76-1* mutant is also defective in meiotic recombination. In budding yeast this process occurs progressively during prophase with DSBs at leptotene, strand exchange intermediates at zygotene/early pachytene, and recombinant products appearing at mid/late pachytene (Padmore et al., 1991; Schwacha and Kleckner, 1997). The finding that *spo76-1* exhibits high levels of Dmc1p and Rad51p foci at leptotene, but a strong deficit of LNs at midzygotene/pachytene, points to a defect in the recombination process between these two stages (i.e., at the same midprophase period where chromosome morphogenesis is especially aberrant). Since many or all stages of meiotic recombination occur in spatial association with the chromosome axes (review in Kleckner, 1996; Roeder, 1997), it is tempting to link the recombination defect with an underlying defect in axial chromosome morphogenesis, specifically one that is related to intersister cohesion. Thus, during meiotic prophase, we could suggest that Spo76p again serves as a transducer of a disruptive chromosomal transition, as during mitotic prometaphase, except that now the

disruptive force is met by the resistance of axial stiffness and is channeled into another type of outcome, one related to recombination. Kleckner (1996) has proposed that the decision as to whether recombinational interactions will yield crossover or noncrossover products is determined at the leptotene/zygotene transition (e.g., at the transition from DSBs to strand exchange products) by the imposition and relief of tension/stress along the chromosomes. It was further proposed that this process has evolved by modification of an analogous progression that normally induces chromosome coiling/folding along mitotic chromosomes at prometaphase so as to minimize intersister connections. This model accounts for all of our results.

Once meiotic chromosomes exit pachytene and pass through the diffuse stage, an additional defect becomes apparent: when chromosomes reemerge at diplotene, sister chromatids are fully separated. Mitotic chromosomes, in contrast, do not exhibit this feature at any stage. Perhaps the additional disruptive forces of the diffuse stage (during which strong chromatin decondensation takes place), which does not occur during the mitotic cycle, acts upon the already compromised *spo76-1* chromosomes to further exaggerate the defect; alternatively, or in addition, Spo76p might play a second, meiosis-specific role at this point (e.g., via effects in the peripheral chromatin where Spo76-GFPp is seen localized).

## Experimental Procedures

### Strains, Cosmids, and Plasmids

Isolation of *spo76-1* is described in Moreau et al. (1985). Culture conditions and both growth M1Gx and regeneration media RG7 were described in Huynh et al. (1986). Subcloning and plasmid preparations utilized pUC19 and *E. coli* strain DH5a (Hanahan, 1983). The HA epitope from plasmid BFG1 (kindly provided by J. Camonis; Chardin et al., 1993) and EGFP from plasmid pEGFP-1 (Clontech) were inserted at a 3′ NsiI site. Details available upon request. All cotransformations were performed with pANscosI (Osiewacz, 1994).

### Transformation of *Sordaria*

Protoplasts were prepared as in Pöggeler et al. (1997) except for the following: glucanex was used instead of novozym; protoplastation buffer was 13 mM Na$_2$HPO$_4$, 45 mM KH$_2$PO$_4$, 600 mM KCl (pH 6.0); transformation buffer was 1 M Sorbitol, 80 mM CaCl$_2$, 10 mM Tris-HCl (pH 7.5). After an overnight regeneration in RG7, protoplasts were added to 7 ml RG7 top agar (45°C) with hygromycin (Boehringer-Mannheim) at a final concentration of 0.4 mg/ml and plated on RG7 plates. After 2–3 days of growth at 23°C, growing colonies were recovered from the selective top layer and individually transferred to fresh M1Gx plates with hygromycin (0.125 mg/ml final concentration). After 14 days at 23°C, the cover plates of the Petri dishes were screened for projections of black spores, and transformants were purified according to Huynh et al. (1986).

### Sequencing

The 6.4 kb complementing fragment was sequenced on both strands using pUC primers (Stratagene) and gene-specific primers (Genosys). Genomic DNA from *spo76-1* and its isogenic wild type was isolated according to Lecellier and Silar (1994) with PCR products sequenced directly (Rosenthal et al., 1993). Transcription start and polyadenylation sites were determined by sequencing the products obtained by, respectively, 5′ and 3′ RACE (Frohman et al., 1988) on poly(A$^+$) RNA from the isogenic wild-type strain using kits (GIBCO–BRL). Total RNA was isolated essentially following Pöggeler et al. (1997): mycelia were ground in 4 M guanidine thiocyanate, 50 mM Tris-HCl (pH 7.8), 10 mM EDTA, 2% sarkosyl, 1 vol % β-mercaptoethanol; RNA was precipitated with LiCl and purified with a RNeasy Plant Mini Kit (Qiagen). Poly(A$^+$) RNA was isolated by oligotex mRNA Mini Kit (Qiagen). All sequence reactions used the DyeDeoxy Terminator, Cycle Sequencing Kit (Applied) and were analyzed on a 373 DNASequencer (Applied).

### Cytology

Cells were processed for immunofluorescence as described in Thompson-Coffe and Zickler (1994). Primary antibodies used were anti-HA 3F10 (Boehringer Mannheim) at 1:4000; MPM-2 (kindly provided by P. N. Rao) at 1:750; and anti-Dmc1 and anti-Rad51 (Bishop, 1994) at 1:1000. Secondary antibodies were Jackson FITC anti-rat (Interchim) or CyTM3 anti-rabbit (Jackson) at a dilution of 1:100 and 1:4000, respectively. Controls included the use of primary or secondary antibodies alone. EGFP was visualized using the Zeiss filter set for FITC and for GFP. In total, four HA and five GFP transformants were analyzed. All cells were observed on a Zeiss Axioplan microscope and images captured by a CCD Princeton camera, or on T-Max 400 film.

For LM, cells were fixed in fresh Lu's fixative (butanol, proprionic acid, and 10% aqueous chromic acid, 9:6:2 v/v). After 10 min of hydrolysis at 70°C, cells were stained in two drops of 2% hematoxylin mixed on the slide with one drop of ferric acetate solution.

For EM, asci were fixed in 2% glutaraldehyde in 0.1 M phosphate buffer (pH 7.2) for 3 hr, postfixed in phosphate-buffered 2% osmium tetroxide for 1 hr, and dehydrated through an alcohol series. Asci were embedded in Epon 812 at 60°C for 24 hr. Serial sections were mounted on Formvar-coated single hole grids and stained in aqueous uranyl acetate for 30 min, followed by lead citrate for 10 min.

### References

Akins, R.A., and Lambowitz, A.H. (1985). General method for cloning *Neurospora crassa* nuclear genes by complementation of mutants. Mol. Cell. Biol. *5*, 2272–2278.

Bailis, J.M., and Roeder, G.S. (1998). Synaptonemal complex morphogenesis and sister-chromatid cohesion require Mek1-dependent phosphorylation of a meiotic chromosomal protein. Genes Dev. *12*, 3551–3563.

Bickel, S.E., Wyman, D.W., and Orr-Weaver, T.L. (1997). Mutational analysis of the *Drosophila* sister-chromatid cohesion protein ORD and its role in the maintenance of centromeric cohesion. Genetics *146*, 1319–1331.

Bishop, D.K. (1994). RecA homologs Dmc1 and Rad51 interact to form multiple nuclear complexes prior to meiotic chromosome synapsis. Cell *79*, 1081–1092.

Chardin, P., Camonis, J.H., Gale, N.W., Van Aelst, L., Schlessinger, J., Wigler, M.H., and Bar-Sagi, D. (1993). Human Sos1: a guanine nucleotide exchange factor for Ras that binds to GRB2. Science *260*, 1338–1343.

Davies, F.M., Tsao, T.Y., Fowler, S.K., and Rao, P.N. (1983). Monoclonal antibodies to mitotic cells. Proc. Natl. Acad. Sci. USA *80*, 2926–2930.

Dawe, R.K., Sedat, J.W., Agard, D.A., and Cande, W.Z. (1994). Meiotic chromosome pairing in maize is associated with a novel chromatin organization. Cell *76*, 901–912.

Denison, S.H., Kafer, E., and May, G.S. (1992). Mutation in the *bimD* gene of *Aspergillus nidulans* confers a conditional mitotic block and sensitivity to DNA damaging agents. Genetics *134*, 1085–1096.

Frohman, M.A., Dush, M.K., and Martin, G.R. (1988). Rapid production of full-length cDNAs from rare transcripts: amplification using a single gene-specific oligonucleotide primer. Proc. Natl. Acad. Sci. USA *85*, 8998–9002.

Geck, P., Szelei, J., Jimenez, J., Sonnenschein, C., and Soto, A.M. (1999). Early gene expression during androgen-induced inhibition of proliferation of prostate cancer cells: a new suppressor candidate on chromosome 13, in the BRCA2-Rb1 locus. J. Steroid Biochem. Mol. Biol. *68*, 41–45.

Gimenez-Abian, J.F., Clarke, D.J., Mullinger, A.M., Downes, C.S., and Johnson, R.T. (1995). A postprophase Topoisomerase II-dependent chromatid core separation step in the formation of metaphase chromosomes. J. Cell Biol. *131*, 7–17.

Guacci, V., Koshland, D., and Strunnikov, A. (1997). A direct link between sister chromatid cohesion and chromosome condensation revealed through analysis of *MCD1* in *S. cerevisiae*. Cell *91*, 47–57.

Hanahan, D. (1983). Studies on transformation of *Escherichia coli* with plasmids. J. Mol. Biol. *166*, 557–580.

Hirano, T. (1999). SMC-mediated chromosome mechanics: a conserved scheme from bacteria to vertebrates? Genes Dev. *13*, 11–19.

Holt, C.L., and May, G.S. (1996). An extragenic suppressor of the mitosis-defective *bimD6* mutation of *Aspergillus nidulans* codes for a chromosome scaffold protein. Genetics *142*, 777–787.

Huynh, A.D., Leblon, G., and Zickler, D. (1986). Indirect intergenic suppression of a radiosensitive mutant of *Sordaria macrospora* defective in sister-chromatid cohesiveness. Curr. Genet. *10*, 545–555.

Kleckner, N. (1996). Meiosis: how could it work? Proc. Natl. Acad. Sci. USA *93*, 8167–8174.

Koshland, D., and Strunnikov, A. (1996). Mitotic chromosome condensation. Annu. Rev. Cell Dev. Biol. *12*, 305–333.

Lecellier, G., and Silar, P. (1994). Rapid methods for nucleic acids extraction from Petri dish-grown mycelia. Curr. Genet. *25*, 122–123.

Losada, A., Hirano, M., and Hirano, T. (1998). Identification of Xenopus SMC protein complexes required for sister chromatid cohesion. Genes Dev. *12*, 1986–1997.

Maguire, M.P., Riess, R.W., and Paredes, A.M. (1993). Evidence from a maize desynaptic mutant points to a probable role of synaptonemal complex central region components in provision for subsequent chiasma maintenance. Genome *36*, 797–807.

Michaelis, C., Ciosk, R., and Nasmyth, K. (1997). Cohesins: chromosomal proteins that prevent premature separation of sister chromatids. Cell *91*, 35–45.

Moens, P.B., and Pearlman, R.E. (1988). Chromatin organization at meiosis. Bioessays *9*, 151–153.

Molnar, M., Bähler, J., Sipiczki, M., and Kohli, J. (1995). The *rec8* gene of *Schizosaccharomyces pombe* is involved in linear element formation, chromosome pairing and sister-chromatid cohesion during meiosis. Genetics *141*, 61–73.

Moore, D.P., and Orr-Weaver, T.L. (1998). Chromosome segregation during meiosis: building an unambivalent bivalent. Curr. Top. Dev. Biol. *37*, 263–299.

Moore, D.P., Page, A.W., Tang, T.T-L., Kerrebrock, A.W., and Orr-Weaver, T.L. (1998). The cohesion protein Mei-S332 localizes to condensed meiotic and mitotic chromosomes until sister chromatids separate. J. Cell Biol. *140*, 1003–1012.

Moreau, P.J.F., Zickler, D., and Leblon, G. (1985). One class of mutants with disturbed centromere cleavage and chromosome pairing in *Sordaria macrospora*. Mol. Gen. Genet. *198*, 189–197.

Nicklas, R.B., Ward, S.C., and Gorbsky, G.J. (1995). Kinetochore chemistry is sensitive to tension and may link mitotic forces to a cell cycle checkpoint. J. Cell Biol. *130*, 929–939.

Osiewacz, H.D. (1994). A versatile shuttle cosmid vector for the efficient construction of genomic cosmid libraries and for the cloning of fungal genes. Curr. Genet. *26*, 87–90.

Padmore, R., Cao, L., and Kleckner, N. (1991). Temporal comparison of recombination and synaptonemal complex formation during meiosis in *S. cerevisiae*. Cell *66*, 1239–1256.

Pöggeler, S., Risch, S., Kuck, U., and Osiewacz, H.D. (1997). Mating-type genes from the homothallic fungus *Sordaria macrospora* are functionally expressed in a heterothallic ascomycete. Genetics *147*, 567–580.

Pukkila, P.J., Shannon, K.B., and Skrzynia, C. (1995). Independent synaptic behavior of sister chromatids in *Coprinus cinereus*. Can. J. Bot. *73* (Suppl.1), S215–S220.

Rechsteiner, M., and Rogers, S.W. (1996). PEST sequences and regulation by proteolysis. Trends Biochem. Sci. *21*, 267–271.

Roeder, G.S. (1997). Meiotic chromosomes: it takes two to tango. Genes Dev. *11*, 2600–2621.

Rosenthal, A., Coutelle, O., and Craxton, M. (1993). Large-scale production of DNA sequencing templates by microtitre format PCR. Nucleic Acids Res. *21*, 173–174.

Schwacha, A., and Kleckner, N. (1997). Interhomolog bias during meiotic recombination: meiotic functions promote a highly differentiated interhomolog-only pathway. Cell *90*, 1123–1135.

Slonimsky, P.P., and Brouillet, S. (1993). A data-base of chromosome III of *Saccharomyces cerevisiae*. Yeast *9*, 941–1029.

Smith, A.V., and Roeder, G.S. (1997). The yeast Red1 protein localizes to the cores of meiotic chromosomes. J. Cell Biol. *136*, 957–967.

Taagepera, S., Rao, P.N., Drake, F.H., and Gorbsky, G.J. (1993). DNA topoisomerase II$\alpha$ is the major chromosome protein recognized by the mitotic phosphoprotein antibody MPM-2. Proc. Natl. Acad. Sci. USA *90*, 8407–8411.

Tang, T.T-L., Bickel, S.E., Young, L.M., and Orr-Weaver, T.L. (1998). Maintenance of sister-chromatid cohesion at the centromere by the *Drosophila* MEI-S332 protein. Genes Dev. *12*, 3843–3856.

Thompson-Coffe, C., and Zickler, D. (1994). How the cytoskeleton recognizes and sorts nuclei of opposite mating type during the sexual cycle in filamentous ascomycetes. Dev. Biol. *165*, 257–271.

Toth, A., Ciosk, R., Uhlmann, F., Galova, M., Schleiffer, A., and Nasmyth, K. (1999). Yeast cohesin complex requires a conserved protein, Eco1p(Ctf7), to establish cohesion between sister chromatids during DNA replication. Genes Dev. *13*, 320–333.

Turcq, B., Denayrolles, M., and Begueret, J. (1990). Isolation of the two allelic incompatibility genes s and S of the fungus *Podospora anserina*. Curr. Genet. *17*, 297–303.

Uhlmann, F., and Nasmyth, K. (1998). Cohesion between sister chromatids must be established during DNA replication. Curr. Biol. *8*, 1095–1101.

Von Wettstein, D., Rasmussen, S.W., and Holm, P.B. (1984). The synaptonemal complex in genetic segregation. Annu. Rev. Genet. *18*, 331–413.

Zickler, D., and Kleckner, N. (1998). The leptotene-zygotene transition of meiosis. Annu. Rev. Genet. *32*, 619–697.

Zickler, D., Moreau, P.J.F., Huynh, A.D., and Slezec, A.M. (1992). Correlation between pairing initiation sites, recombination nodules and meiotic recombination in *Sordaria macrospora*. Genetics *132*, 135–148.

**EMBL Accession Number**

The EMBL accession number for the *SPO76* sequence is AJ009934.